

An experiment to observe the intensity and phase structure of Laguerre–Gaussian laser modes

M. Padgett, J. Arlt, N. Simpson, and L. Allen

Citation: *American Journal of Physics* **64**, 77 (1996); doi: 10.1119/1.18283

View online: <http://dx.doi.org/10.1119/1.18283>

View Table of Contents: <http://scitation.aip.org/content/aapt/journal/ajp/64/1?ver=pdfcov>

Published by the [American Association of Physics Teachers](#)

Articles you may be interested in


[The role of Gouy phase on the mechanical effects of Laguerre-Gaussian light interacting with atoms](#)
AIP Conf. Proc. **1742**, 030009 (2016); 10.1063/1.4953130


[Tight focusing of higher orders Laguerre-Gaussian modes](#)
AIP Conf. Proc. **1724**, 020021 (2016); 10.1063/1.4945141

[Optical limiting using Laguerre-Gaussian beams](#)
Appl. Phys. Lett. **91**, 201110 (2007); 10.1063/1.2814886

[X-ray interference in quantum-well laser structures](#)
J. Appl. Phys. **65**, 1036 (1989); 10.1063/1.343064

[Growth of periodic structures in pyrolytic laser-deposited SiC](#)
J. Appl. Phys. **60**, 470 (1986); 10.1063/1.337798




2016 Quadrennial Physics Congress

**The perfect venue
for REU students to present
their research.**

Info

28-Nuclear Radiation (Department of Physics & Astronomy, Dickinson College, October 1994), Version 2.0, Unit 28, p. 26.

⁷Nicholas Lumb, "Radon in buildings: A simple detection method," *Phys. Educ.* **24**, 175–177 (1989).

⁸The air sampler, Dwyer Instruments, Michigan City, was essentially a vacuum cleaner motor with a 15×20 cm intake aperture covered with a grill work over which standard filter paper could be placed. The exhaust aperture was fitted with a pitot tube and water manometer for determining volume of air flow.

⁹Reference 1, p. 33.

¹⁰Michael J. Kraft, Springfield, MO, a local radon monitoring specialist.

¹¹A. V. Nero, M. B. Schwehr, W. W. Nazaroff, and K. L. Reozan, *Science* **234**, 992–997 (1986).

¹²B. L. Cohen, "A national survey of 222 Rn in U. S. homes and correlating factors," *Health Phys.* **51**, 175–183 (1986).

¹³H. W. Alter and R. H. Oswald, "Nationwide distribution of indoor radon measurements: a preliminary data base," *J. Pollution Control Assoc.* **37**, 227–231 (1987).

An experiment to observe the intensity and phase structure of Laguerre–Gaussian laser modes

M. Padgett, J. Arlt, and N. Simpson

J. F. Allen Research Laboratories, Department of Physics and Astronomy, The University of St. Andrews, North Haugh, St. Andrews, Fife, KY16 9SS, United Kingdom

L. Allen

Department of Physics, University of Essex, Colchester, Essex CO4 3SQ, United Kingdom

(Received 14 June 1994; accepted 3 April 1995)

We outline an easily reproduced experiment that allows the student to investigate the intensity and phase structure of transverse laser modes. In addition to discussing the usual Hermite–Gaussian laser modes we detail how Laguerre–Gaussian laser modes can be obtained by the direct conversion of the Hermite–Gaussian output. A Mach–Zehnder interferometer allows the phase structure of the Laguerre–Gaussian modes to be compared with the phase structure of a plane wave with the same frequency. The resulting interference patterns clearly illustrate the azimuthal phase dependence of the Laguerre–Gaussian modes, which is the origin of the orbital angular momentum associated with each of them. © 1996 American Association of Physics Teachers.

I. INTRODUCTION

Lasers form a key topic within an increasing number of undergraduate physics and optoelectronic degrees. This paper presents an easily reproduced experiment that allows the student to investigate the amplitude and phase structure of various transverse laser modes. In general, transverse laser modes are best described by a product of a Hermite polynomial and a Gaussian and are known as Hermite–Gaussian (HG) modes. However, in this paper we show how other modes can be generated and their phase distribution analyzed. Specifically, we present results relating to the Laguerre–Gaussian (LG) transverse laser modes. Laguerre polynomials are more frequently encountered within quantum mechanics as the radial term in the solution to Schrödinger's time-independent wave equation for a harmonic oscillator potential (e.g., the hydrogen atom problem). As in the quantum mechanical example the presence of an azimuthal phase term may be interpreted as indicating the presence of orbital angular momentum, hence the current interest in these unusual laser modes^{1–4}

II. LONGITUDINAL AND TRANSVERSE MODES WITHIN LASER OSCILLATORS

All lasers essentially consist of a gain material within which stimulated emission amplifies the light and an optical

resonator to provide the feedback needed to form an oscillator. The electromagnetic field within the laser resonator must satisfy a number of boundary conditions. In the steady state, there is the requirement that it reproduce itself in phase after one round trip of the laser cavity. This gives rise to the longitudinal mode structure of the laser. For a two-mirror linear cavity of optical length L , the operating wavelength of the laser, λ , must satisfy the equation

$$m(\lambda/2) = L, \quad (1)$$

where m is an integer.

The second boundary condition constrains the transverse nature of the electromagnetic field. In free space, there is a requirement that the electromagnetic field falls to zero away from the axis of the laser cavity. This gives rise to the transverse mode structure within the laser cavity and the observed intensity profile of the laser output. The analytical form of the allowed laser modes must satisfy these conditions and be a scalar solution to the paraxial limit of Maxwell's wave equation. (The paraxial limit assumes that the light diverges at only a small angle with respect to the optical axis of the system.⁵) This requires both the field amplitude and its derivative to fall to zero at a large distance from the axis of the cavity.

The rectangularly symmetric HG modes are described in part by the product of two-independent Hermite polynomi-

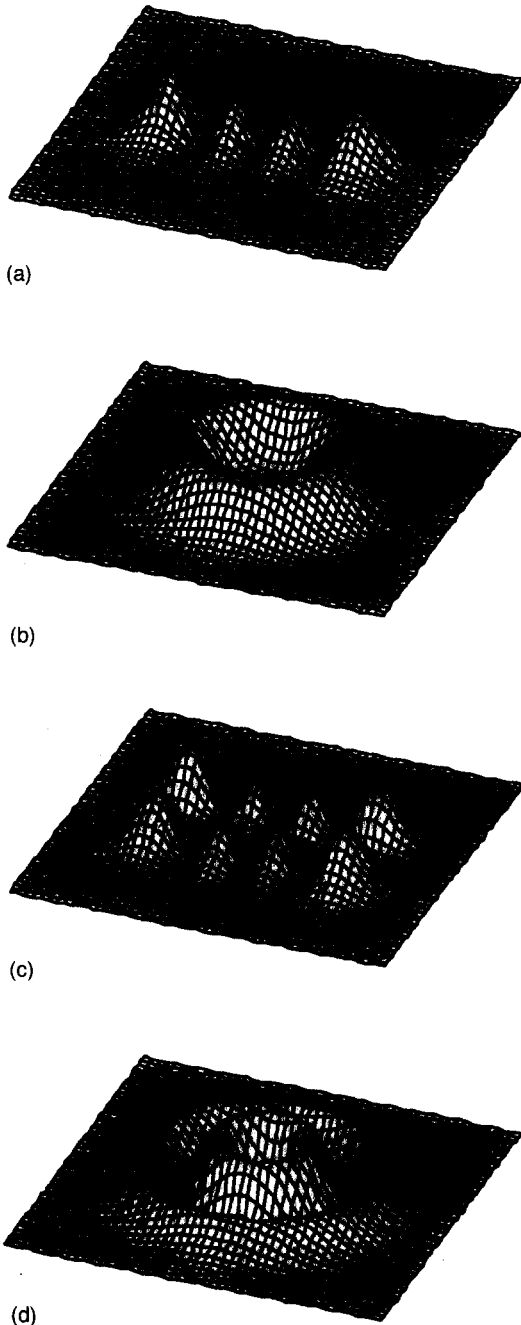


Fig. 1. Intensity ($|E|^2$) distribution of (a) a Hermite-Gaussian mode $m=3$, $n=0$, (b) a Laguerre-Gaussian mode $l=3$, $p=0$, (c) a Hermite-Gaussian mode $m=3$, $n=1$, and (d) a Laguerre-Gaussian mode $l=2$, $p=1$.

als, for the field distribution in the x and y directions, respectively. They are characterized by the integer subscripts m and n which give the order of the two polynomials. The values of m and n correspond to the number of nodes in the electromagnetic field. For example, the $HG_{3,1}$ mode has three field nodes in the x direction and one in the y direction [See Figs. 1(a) and 1(c)].

The circularly symmetric LG modes are similarly described by a single Laguerre polynomial with the superscript l and the subscript p . The index l gives the number of 2π cycles of phase in the azimuthal direction around the circumference of the mode, while $p+1$ gives the number of nodes across the radial field distribution. The LG_1^2 mode has a 4π

phase variation around the circumference of the mode and two radial nodes one of which is on axis. [See Figs. 1(b) and 1(d)].

As frequently encountered within quantum mechanics, it is the symmetry of the potential well and associated boundary conditions that determines the set of functions that most conveniently describes the eigenfunctions of the system. In the case of the simple harmonic oscillator, rectangular symmetry gives rise to HG eigenfunctions and circular symmetry results in LG eigenfunctions. In the case of a laser system, it would seem probable that given circular mirrors, the LG functions would provide the most accurate description of the transverse modes in a real laser, but this is not the case. Slight asymmetries in the laser cavity such as the inclusion of a Brewster window give rise to rectangular symmetry which results in a product of Hermite polynomials providing a more appropriate description. A full description with many examples of transverse laser modes can be found in Siegman's book.⁶ As an example of what the eigenfunctions look like, the field amplitudes, E , transverse to the direction of propagation for the $HG_{3,1}$ and LG_1^2 modes, by way of example, are given by

$$\begin{aligned}
 E(HG_{3,1}) &\propto \exp\left(-ik \frac{(x^2+y^2)}{2R}\right) \\
 &\quad \times \exp\left(\frac{-(x^2+y^2)}{\omega^2}\right) H_3\left(\frac{\sqrt{2}x}{\omega}\right) H_1\left(\frac{\sqrt{2}y}{\omega}\right) \psi(z), \\
 E(LG_1^2) &\propto \exp\left(-ik \frac{r^2}{2R}\right) \exp\left(\frac{-r^2}{\omega^2}\right) \left(\sqrt{2} \frac{r}{\omega}\right)^2 \\
 &\quad \times L_1^2\left(\frac{2r^2}{\omega^2}\right) \exp(-2i\phi) \psi(z),
 \end{aligned} \tag{2}$$

where R is the radius of curvature of the near spherical wave front, k is the wave number of the electromagnetic wave, while x , y , and r are the transverse positions and radii within the beam, ϕ is the azimuthal angle within the beam, and ω is the beam radius at which the Gaussian term falls to $1/e$ of its on axis value. In both of the above expressions, the first factor relates to the phase change that results from the curvature of the wave front, and the factor $\psi(z)$ is the Gouy phase which we shall consider in detail later. The polynomials in these cases are

$$\begin{aligned}
 H_3\left(\frac{\sqrt{2}x}{\omega}\right) &= 8\left(\frac{\sqrt{2}x}{\omega}\right)^3 - 12\left(\frac{\sqrt{2}x}{\omega}\right), \\
 H_1\left(\frac{\sqrt{2}y}{\omega}\right) &= 2\frac{\sqrt{2}y}{\omega}
 \end{aligned}$$

and

$$L_1^2\left(\frac{2r^2}{\omega^2}\right) = 3 - \frac{2r^2}{\omega^2}. \tag{3}$$

III. THE GENERATION OF HIGH-ORDER TRANSVERSE LASER MODES

In most uses of a laser, the multilobed or multiringed nature of a high-order transverse mode is undesirable. Steps are taken to force the laser to oscillate in the fundamental mode $m=0$, $n=0$, the amplitude of which has the form of a simple Gaussian centered on axis. As a laser will tend to oscillate in the transverse mode for which the losses are lowest, the fun-

damental mode is often preferentially selected by the inclusion of an aperture into the cavity. Similarly, if one of the higher-order HG modes is in fact required, then this is most simply achieved by inserting a cross wire into the laser cavity with the wires aligned with the nodes of the desired mode. However, obtaining a pure LG is not so easy because the azimuthal phase term can be either clockwise or anticlockwise. The two modes have identical intensity distributions and a simple mask or aperture is therefore not sufficient to select one mode in preference to the other. Although a LG laser output has been reported, see for example the recent work by Harris *et al.*,⁷ the experimental difficulties are beyond what can be expected of a teaching laboratory and we show an alternative way in which such modes may be investigated.

Recent work by Beijersbergen *et al.*⁸ has demonstrated, following the work of Tamm and Weiss⁹ on low-order modes, that there is an extra-cavity way to obtain pure LG modes of any order. A mode converter consisting of two cylindrical lenses can transform the HG output of a conventional laser into the corresponding LG mode. In the experiment described here, we convert the HG output of a He-Ne laser into the desired LG mode and investigate the relative phase structure by superposing the LG mode on the HG mode derived from the same laser source. The resulting interference pattern allows the direct observation of the azimuthal phase dependence of the LG modes.

IV. THE OPERATING PRINCIPLE OF THE MODE CONVERTER

The HG and LG modes both form complete sets of solutions to the paraxial wave equation. Any arbitrary paraxial distribution can be described as a superposition of HG or LG terms with the appropriate weighting and phase factors. It follows that an LG mode can be described as a superposition of various HG modes weighted and phased accordingly, and vice versa. It has been shown^{1,10} surprisingly recently, that the relationship between the HG and LG modes is comparatively simple, and examples detailing how various LG modes can be synthesized from combinations of HG modes are presented in Ref. 8. Figure 2 shows how a HG_{1,0} mode rotated at 45° to the *x*-*y* axis is equivalent to the sum of a HG_{1,0} and HG_{0,1} modes and how these two modes are related to the LG₀¹ mode. Specifically, the LG₀¹ can be formed by the superposition of the HG_{1,0} and the HG_{0,1} modes with a phase difference of $\pi/2$.

The propagation of laser beams with a HG or LG structure can be described in the usual language of Gaussian beams (see Ref. 5). The radius of the beam, ω , at which the Gaussian factor in the expression for the electric field falls to $1/e$ of its on axis value and the radius of curvature, R , of the near spherical wave fronts are given by,

$$\omega^2(z) = \frac{2(z_r^2 + z^2)}{kz_r},$$

$$R(z) = \frac{(z_r^2 + z^2)}{z}, \quad (4)$$

where the quantity z_r is the Rayleigh range and k is the wave number of the electromagnetic wave. The position $z=0$ corresponds to the smallest beam radius, and this position is

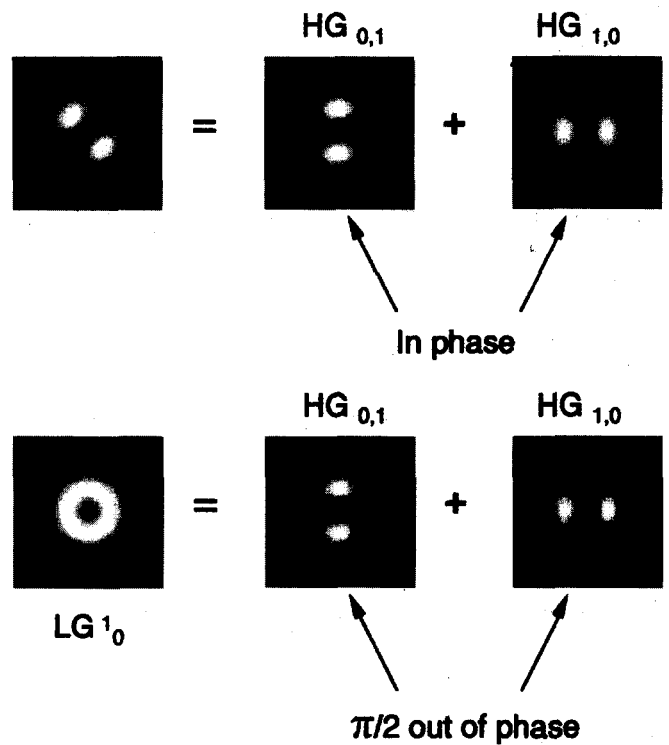


Fig. 2. The LG₀¹ mode can be formed by the superposition of the HG_{1,0} and the HG_{0,1} modes with a phase delay of $\pi/2$.

referred to as the beam waist. The radius of the beam waist, ω_0 , is related to the Rayleigh range by

$$\omega_0^2 = 2z_r/k. \quad (5)$$

In the vicinity of the beam waist, a Gaussian beam experiences a phase shift compared to that of a plane wave of the same frequency. This phase shift ψ is termed the Gouy phase.¹¹ For the simple case of a HG mode, described by mode indices m and n in the *x* and *y* directions respectively, and with identical Rayleigh ranges in the *x*-*z* and *y*-*z* planes, $z_{r(x-z)} = z_{r(y-z)}$, the Gouy phase is given by

$$\psi(z) = (n + m + 1) \arctan(z/z_r), \quad (6)$$

while for a LG mode the phase is written

$$\psi(z) = (2p + l + 1) \arctan\left(\frac{z}{z_r}\right), \quad (7)$$

where z is the distance along the axis from the beam waist in each case. If the Gaussian beam is focused by a cylindrical lens then the situation becomes more complex as the Rayleigh ranges in the *x*-*z* and *y*-*z* planes are not equal, $z_{r(x-z)} \neq z_{r(y-z)}$. Such a beam is termed an elliptical Gaussian beam and the corresponding Gouy phase shift for the HG_{*m,n*} mode is given by

$$\psi(z) = \left(m + \frac{1}{2}\right) \arctan\left(\frac{z}{z_{r(x-z)}}\right) + \left(n + \frac{1}{2}\right) \arctan\left(\frac{z}{z_{r(y-z)}}\right). \quad (8)$$

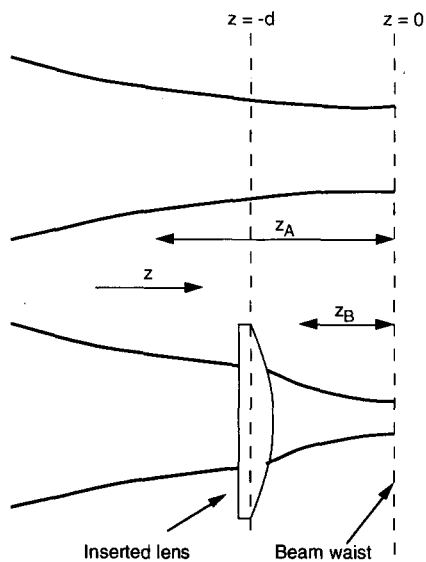


Fig. 3. A lens inserted into a Gaussian beam with a Rayleigh range z_A can be selected to change the Rayleigh range to z_B while leaving the position of the beam waist unaltered.

It is the Gouy phase shift in the presence of a cylindrical lens that forms the basis of the mode converter.

Consider a Gaussian beam traveling in the z direction with a Rayleigh range z_A and a beam waist at $z=0$. A lens inserted at $-d$ would change the radius of curvature of the beam and it proves possible to select a focal length which changes the Rayleigh range from z_A to z_B without affecting the position of the beam waist (see Fig. 3). A second, identical, lens positioned at $+d$ would change the Rayleigh range back to z_A . If the lenses are cylindrical, aligned with their axes parallel to the x direction, then only the Rayleigh range in the $y-z$ plane is affected and consequently in the region between the lenses $z_r(x-z)$ is no longer equal to $z_r(y-z)$ and the beam waist is elliptical (see Fig. 4). The differing Rayleigh ranges in the $x-z$ and $y-z$ planes means that in transmission through the lens pair, the $HG_{m,n}$ and $HG_{n,m}$ ($m \neq n$) modes will undergo different Gouy phase shifts. For the generation of the LG_0^1 mode, we require that this phase difference be

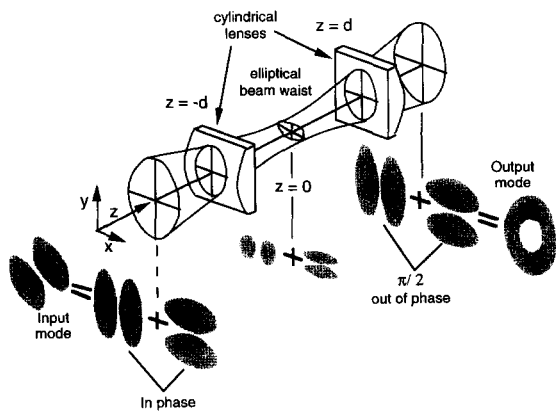


Fig. 4. The cylindrical lens mode converter. If the input $HG_{1,0}$ mode is oriented at 45° with respect to the cylinder axis of lens the mode is converted into the LG_0^1 mode.

$\pi/2$. Beijersbergen *et al.* show that this occurs when the separation, $2d$, of the cylindrical lenses of focal length f is given by

$$2d = f \sqrt{2}, \quad (9)$$

and the Rayleigh range, z_r , of the incident beam is given by

$$z_r = (1 + 1/\sqrt{2})f. \quad (10)$$

The correct Rayleigh range of the beam entering the mode converter is established using an additional spherical lens of an appropriate focal length, prior to the mode converter, positioned to form a beam waist at $z=0$. For a diverging input beam, with a wave-front radius of R_i and of radius ω , the required focal length, f_{in} , of the input lens is given by

$$\frac{1}{f_{in}} = \frac{\sqrt{2k\omega^2 z_r - 4z_r^2}}{k\omega^2 z_r} + \frac{1}{R_i}, \quad (11)$$

where k is the wave number of the light.

It can be shown that in addition to the transformation of the $HG_{1,0}$ mode, a mode-converter of the above design will transform any $HG_{m,n}$ mode, rotated at 45° to the axis of the lens, into the corresponding LG_p^l mode with $l = |m - n|$ and $p = \min(m, n)$.

V. EXPERIMENTAL APPARATUS

The design of the mode converter used in this work is based on the simple equations given in the previous section and has the following specifications:

- 25.4 mm focal length cylindrical lenses (e.g., Newport CKX025¹²),
- 35.9 mm lens separation (between the principal planes) and an input beam with a Rayleigh range of 43.3 mm.

The lenses are mounted with their plane faces cemented to a 19 mm long tube to set the correct separation of their principal planes.

The optimum focal length for the input lens can be calculated from the diameter of the input beam and its wave-front curvature. However, in practice it is simpler to experiment with a number of different focal lengths and select the one that gives the best results. In our case, a single lens of 250 mm focal length is used to focus the output of the HeNe laser into the mode converter.

For the laser source, we use an unmounted He-Ne tube with a Brewster window and an external output coupler.¹³ By positioning the output coupler 100 mm from the Brewster window, an $x-y$ translation stage carrying a crosswire (made from 10 μm diam tungsten wire) can be inserted into the laser cavity. With careful adjustment of the cross wire and alignment of the output coupler, the student can force the laser to oscillate in a variety of higher-order HG modes.

In order to observe the phase structure of the LG modes it was necessary to extend the experimental arrangement beyond that of the mode converter, as shown in Fig. 5. The experimental arrangement is based on a Mach-Zehnder interferometer, with the mode converter and input lens ($f=250$ mm) in one arm and a beam expansion telescope in the other. The purpose of the lens ($f=160$ mm) after the mode converter is to form a second beam waist outside the interferometer, so that the mode structure can be examined at various positions either side of a beam waist. The beam expansion telescope consists of two lenses ($f=40$ mm and $f=300$ mm) to give an expanded, collimated output beam. This beam is

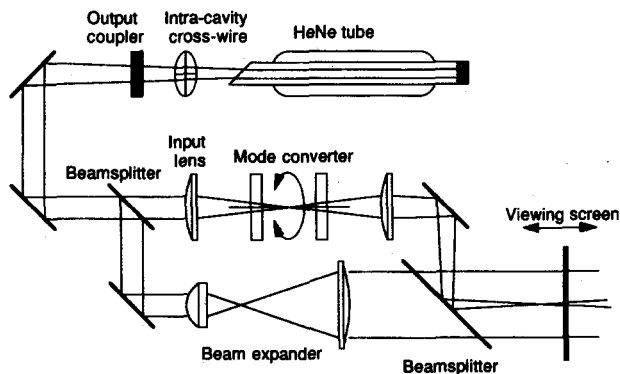


Fig. 5. The experimental arrangement for the observation of the intensity and phase structure of Laguerre-Gaussian transverse laser modes.

an expanded form of the input HG mode. Although having a Hermite Gaussian intensity profile, the large Rayleigh range now achieved for the mode results in a near-planar wave front that acts as a phase reference for the examination of the LG modes.

VI. EXPERIMENTAL OBSERVATION OF THE INTENSITY AND PHASE STRUCTURE OF LG MODES

Initial experiments can be completed with the beam expander arm blocked off. The results presented in Ref. 8 can be repeated; namely after selecting a high-order HG mode from the laser the student can examine the intensity distribution of the beam after it is transmitted by the mode converter. If the cylindrical lenses are rotated about the optical axis so that the axis of the cylinders are at 0° or 90° to the input HG mode then the transmitted light is also an HG mode. If, however, they are rotated to lie at 45° , the input $HG_{n,m}$ mode is transformed to the corresponding LG_p^l mode ($l = |m - n|$ and $p = \min(m, n)$).

After the various intensity patterns have been observed, the student can superimpose the expanded HG mode, aligned so that the LG mode falls within one of the greatly expanded lobes, and the resulting interference pattern can be observed. The expanded HG mode acts as a plane-wave reference and the observed fringes reveal the relative phase variations of the HG or LG mode in question.

Figure 6 shows the intensity distributions and interference patterns of a $HG_{3,0}$ mode and the corresponding LG_0^3 mode at various positions about the beam waist. These intensity distributions can be observed simply by placing a screen in the beam path. For the purpose of publication and student reports, permanent record of the intensity distributions can be obtained by directly exposing a CCD array interfaced to a framegrabbing card running on a desktop computer. Subsequently, the interferogram image can be printed or transferred into a variety of applications running on the same computer.

As can be seen from the figure, at the beam waist the 6π phase change around the circumference of the LG_0^3 mode gives rise to three dark radial fringes. Away from the beam waist, spiral fringes are observed. These arise from the combination of the radial phase variation due to wave-front curvature, and the tangential phase variation due to the azimuthal phase dependence. The sense of the spiral is reversed on either side of the waist in accordance with the curvature

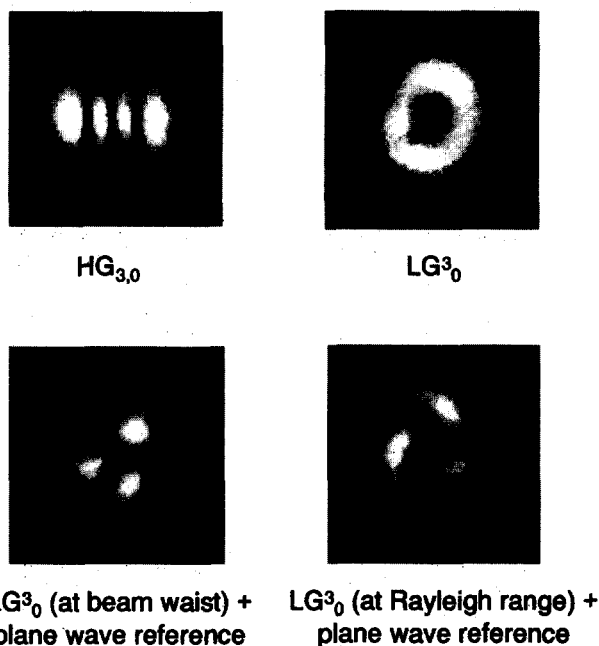


Fig. 6. Photographs of the Hermite-Gaussian $HG_{3,0}$ mode, the transformed Laguerre-Gaussian LG_0^3 mode and interferograms between the LG_0^3 mode and a plane wave.

of the wave fronts. In addition, the sense of the spirals can be reversed by changing the sense of the azimuthal phase variation. This is most readily achieved by rotating the mode converter about the optical axis by 90° (i.e., from $+45^\circ$ to -45° with respect to the input mode).

Figure 7 shows the intensity and interference patterns ob-

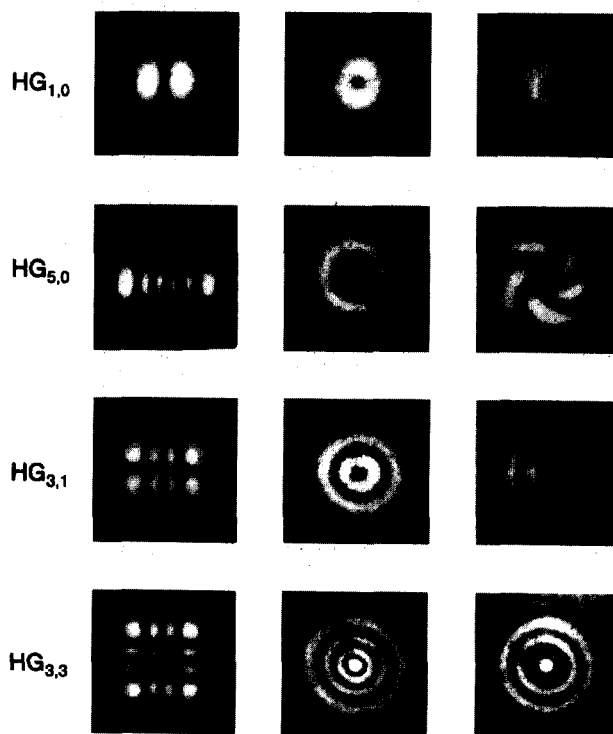


Fig. 7. Photographs of a number of Hermite-Gaussian laser modes, the corresponding Laguerre-Gaussian modes and interferograms between the Laguerre-Gaussian modes and a plane-wave reference.

tained for several higher-order HG and LG modes. In all cases the number of radial fringes is equal to l (i.e., $|m-n|$) and the number of radial nodes is equal to $p+1$ [i.e., $\min(m,n)+1$]. For the LG modes with multiple ring amplitudes (e.g., the LG_1^2 , which is obtained from the $HG_{3,1}$), the azimuthal position of the fringe maxima and minima are reversed between successive rings, corresponding to the change of phase of the Laguerre–Gaussian distribution. Note also that in the special case of $m=n$ there is an on axis intensity for the LG mode but no azimuthal phase dependence and hence the fringes are circular and not spiral. The radii of the fringes can be calculated from the wave-front curvature of the beam and are analogous to Newton’s rings.

VII. CONCLUSIONS

This paper presents an easily reproduced experiment with which the student can investigate the intensity and phase structure of various transverse laser modes. In addition to the standard Hermite–Gaussian laser modes we detail how Laguerre–Gaussian laser modes can be obtained by the direct conversion of the Hermite–Gaussian laser output using a mode converter utilizing the Gouy phase shift in the region of an elliptical beam waist. Using a Mach-Zehnder interferometer, the phase structure of the Laguerre–Gaussian modes can be compared with that of a plane wave of the same frequency.

One of the current sources of interest in the LG laser modes is that they are predicted to carry orbital angular momentum in addition to the spin momentum associated with the polarization state of the photons.¹ By superimposing the LG mode with a plane-wave reference, the resulting interference patterns clearly illustrate the azimuthal phase dependence of the Laguerre–Gaussian modes which is the origin of the orbital angular momentum associated with these modes.

ACKNOWLEDGMENT

Miles Padgett is a Royal Society of Edinburgh Research Fellow.

- ¹L. Allen, M. W. Beijersbergen, R. J. C. Spreeuw, and J. P. Woerdman, “Orbital angular momentum of light and the transformation of Laguerre-Gaussian laser modes,” *Phys. Rev. A* **45**, 8185–8189 (1992).
- ²M. W. Beijersbergen, M. Kristensen, and J. P. Woerdman, “Spiral phase-plate used to produce helical wavefront laser beams,” *Technical Digest, CLEO, Europe, CFA5* (1994).
- ³M. J. Padgett and L. Allen, “The Poynting vector in Laguerre-Gaussian modes,” submitted to *Optic Commun.*
- ⁴M. Babiker, W. L. Power, and L. Allen, “Light-induced torque on moving atoms,” *Phys. Rev. Lett.* **73**, 1239–1242 (1994).
- ⁵For example see R. Guenther, *Modern Optics* (Wiley, New York, 1990), pp. 336–343; A. E. Siegman, *Lasers* (University Science Books, Mill Valley, 1986), Sec. 7.3, pp. 276–279.
- ⁶A. E. Siegman, *Lasers* (University Science Books, Mill Valley, 1986), Sec. 17.5, pp. 685–695.
- ⁷M. Harris, C. A. Hill, and J. M. Vaughan, “Optical helices and spiral interference fringes,” *Opt. Comm.* **106**, 161–166 (1994).
- ⁸M. W. Beijersbergen, I. Allen, H. E. I. O. van der Veen, and J. P. Woerdman, “Astigmatic laser mode converters and transfer of orbital angular momentum,” *Opt. Comm.* **96**, 123–132 (1993).
- ⁹Chr. Tamm and C. O. Weiss, “Bistability and optical switching of spatial patterns in a laser,” *J. Opt. Soc. Am. B* **7**, 1034–1038 (1990).
- ¹⁰S. Danakas and P. K. Aravind, “Analogies between two optical systems (photon beam splitters and laser beams) and two quantum systems (the two-dimensional oscillator and the two-dimensional hydrogen atom),” *Phys. Rev. A* **45**, 1973–1977 (1992).
- ¹¹A. E. Siegman, *Laser* (University Science Books, Mill Valley, 1986), Sec. 17.4, pp. 682–685.
- ¹²Newport Optics Catalogue.
- ¹³Melles Griot, He–Ne plasma tube 05LHB570, Output coupler L01002-1.

On a simple experiment on the free rotation of a ruler and other laminas

A. Amengual

Departament de Física, Universitat de les Illes Balears, E-07071 Palma de Mallorca, Spain

(Received 15 August 1994; accepted 28 April 1995)

The torque-free rotation of a solid body is unstable about the axis with the intermediate principal moment of inertia. Such an instability can be shown with a simple experiment using a ruler. In this work, the equations of Euler are integrated and the orientation of the ruler, referred to the laboratory reference frame, determined as a function of time. This allows a beautiful comparison between the observed rotation of the ruler and the theory behind it. © 1996 American Association of Physics Teachers.

I. INTRODUCTION

The dynamics of spinning objects can be introduced to physics students by using simple but very stimulating demonstrations. Tops and gyroscopes display many *unexpected* and challenging movements, one can also use some toys,^{1–3}

some simple setups^{4–6} or a common object such as a football,⁷ all of them serve to illustrate and introduce several topics of rigid motion, either torque-free or not.

In this paper, we analyze a very simple experiment related to the free rotation of solid bodies. It is known that a body